UCLA
COMPUTATIONAL AND APPLIED MATHEMATICS

Two-color Fourier Analysis of the Multigrid Method with Red/Black Gauss-Seidel Smoothing*

C.-C. Jay Kuo
Bernard C. Levy

January 1988

CAM Report 88-02

Department of Mathematics
University of California, Los Angeles
Los Angeles, CA. 90024-1555

January 21, 1988

Two-color Fourier Analysis of the Multigrid Method with Red/Black Gauss-Seidel Smoothing*

C.-C. Jay Kuo†

Bernard C. Levy††

Abstract

A two-color Fourier analytical approach is proposed to analyze the multigrid method which employs the red/black Gauss-Seidel smoothing iteration for solving the Poisson equation. In this approach, Fourier components in the high frequency region are folded into the low frequency region so that the coupling between the low and high Fourier components is transformed into a coupling between components of red and black computational waves in the low frequency region. We show that the two-color two-grid method asymptotically reduces to a one-color two-grid method whose physical mechanism is more transparent than for its original two-color form. The two-color Fourier analysis is also used to design variants of the standard multigird algorithm.

Key Words: Fourier analysis, multigrid methods, red/black relaxation, SOR iteration, two-grid analysis.

AMS(MOS) subject classification: 65N20, 65F10

---

* This work was supported in part by the Department of Energy under contract DE-FG03-87ER25037 and by the National Science Foundation under contract NSF-DMS87-14612.

† Department of Mathematics, University of California, Los Angeles, CA 90024.

†† Department of Electrical and Computer Engineering, University of California, Davis, CA 95616.

1 Introduction

It is well known that the multigrid method which employs the red/black Gauss-Seidel smoothing iteration provides a very effective way of solving elliptic PDEs [3][9]. The red/black relaxation scheme is also attractive for parallel computation [1][2][7]. However, the mechanism of this method is not as transparent as for methods which use other types of smoothers such as the damped Jacobi iteration [6][9]. Through the red/black Gauss-Seidel iteration, low and high frequency components of the solution are coupled together, so that some high frequency components are in fact primarily computed by the coarse-grid correction procedure. Therefore, it is more difficult to give a physical explanation of this phenomenon. A two-grid analysis of this method for a model problem consisting of the Poisson equation on the unit square with Dirichlet boundary conditions has been performed by Stüben and Trottenberg [9]. The objective of this paper is to use a variant of Fourier analysis called the *two-color* Fourier analysis to provide more insight into the mechanism of this method.

The red/black relaxation operator and the restriction and interpolation operators are linear *periodic* operators. A straightforward Fourier analysis does not apply since they are spatially dependent. Nevertheless, the *periodic* property can be exploited to reformulate the conventional Fourier analysis as a two-color Fourier analysis [7]. From this new viewpoint, components in the high frequency region are folded into the low frequency region so that there exist two, i.e. red and black, computational waves in the low frequency region. The coupling between the low and high conventional Fourier components is therefore transformed into a coupling between red and black computational waves with the same frequency in the low frequency region. With this new Fourier tool, the spectral representation of every operator in the two-grid analysis can be easily derived and interpreted. Then, we show that the two-color two-grid method asymptotically reduces to a one-color two-grid method which is easier to analyze than in its original two-color form. Although our analysis is different from

that of Stüben and Trottenberg [9], it turns out, without surprise, that they are mathematically equivalent and lead to the same results.

The two-color Fourier analysis not only serves as an analytical tool but is also a useful design tool. This is particularly evident for the 1D problem, for which the two-color two-grid Fourier analysis can be used to design a fast direct method. For the 2D problem, some variants are also derived to improve the performance of the standard multigrid method with red/black Gauss-Seidel smoothing.

This paper is organized as follows. The 1D problem is studied in Section 2. The analysis and design of the 2D two-grid method is presented in Section 3. Concluding remarks are given in Section 4.

2. Analysis and design of 1D multigrid algorithm

Consider a $(h,2h)$ two-grid method for solving the discretized 1D Poisson equation on Ω=[0,1] with boundary values $u(0)$ and $u(1)$, i.e.

$$\frac{1}{h^2}\,(\,u_{n-1} - 2\,u_n + u_{n+1}\,) = f_n \quad , \qquad n = 1, 2, \cdots, N-1 \,, \tag{2.1}$$

where u_n is the estimate of $u(nh)$, h is the grid spacing, and $N = \frac{1}{h}$ is even. The difference between the exact solution $\overline{u}_n$ and the estimate u_n is the error $e_n = u_n - \overline{u}_n$. For a two-grid method, the error equation can be written as

$$\mathbf{e}^{new} = M_h^{2h}\mathbf{e}^{old} \,,$$

where $\mathbf{e} = (e_1, \cdots, e_{N-1})^T$ and M_h^{2h} is the two-grid iteration operator [9],

$$M_h^{2h} = S_h^{\nu_2}\, K_h^{2h}\, S_h^{\nu_1} \,,$$

where S_h is the smoothing operator (smoother) for the h-grid Ω_h, ν_1 and ν_2 are the numbers of presmoothing and postsmoothing iterations, and K_h^{2h} is the coarse-grid correction operator (coarse-grid corrector)

$$K_h^{2h} = I_h - I_{2h}^h L_{2h}^{-1} I_h^{2h} L_h \,,$$

and where I_h, I_{2h}^h, L_{2h}, I_h^{2h}, L_h are the identity, interpolation, coarse-grid Laplacian, restriction, and fine-grid Laplacian operators respectively.

2.1 Two-color Fourier analysis

The analysis of M_h^{2h} is often performed in the frequency domain so that we consider the coefficients $\hat{e}_k$, $1 \le k \le N-1$, of the Fourier expansion

$$e_n = \sum_{k=1}^{N-1} \hat{e}_k \sin(k\pi nh) \,. \tag{2.2}$$

The decomposition (2.2) is particularly convenient for understanding multigrid methods which employ the damped Jacobi smoothing iteration [9]. However, when we use the red/black Gauss-Seidel smoothing iteration, the Fourier components $\hat{e}_k$ and $\hat{e}_{N-k}$ are coupled together. In this paper, a modified Fourier analysis is introduced to analyze this type of smoother. As usual, we call grid points with even and odd indices the red

and black points. Errors at red and black points form red and black sequences, which can be expanded in Fourier series as

$$e_n = \sum_{k=1}^{\frac{N}{2}-1} \hat{r}_k \sin(k\pi nh) \quad , \quad n \quad \text{even} \, , \tag{2.3a}$$

$$e_n = \sum_{k=1}^{\frac{N}{2}} \hat{b}_k \sin(k\pi nh) \quad , \quad n \quad \text{odd} \, . \tag{2.3b}$$

It is straightforward to see that the Fourier components of the red and black sequences are related to the Fourier components of the complete sequence e_n via

$$\begin{bmatrix} \hat{r}_k \\ \hat{b}_k \end{bmatrix} = \frac{1}{2} \begin{bmatrix} 1 & -1 \\ 1 & 1 \end{bmatrix} \begin{bmatrix} \hat{e}_k \\ \hat{e}_{N-k} \end{bmatrix}, \quad 1 \le k \le \frac{N}{2}-1 \quad \text{and} \quad \hat{b}_{\frac{N}{2}} = \hat{e}_{\frac{N}{2}} \, .$$

The decomposition (2.3), called the two-color Fourier analysis, is particularly convenient for operators operating on grid points on a periodical basis.

For example, consider a Jacobi relaxation operation operating at the red points only,

$$e_n^{new} = \frac{1}{2}[\, e_{n-1}^{old} + e_{n+1}^{old} \,] \qquad n \quad \text{even} \, , \qquad e_n^{new} = e_n^{old} \qquad n \quad \text{odd} \, .$$

In the spectral domain, the matrix representation of this iteration describing its action on $(\, \hat{r}_k \, , \, \hat{b}_k \,)^T$, $1 \le k \le \frac{N}{2}-1$, is given by

$$\hat{S}_{h,r}(\theta) = \begin{bmatrix} 0 & \cos\theta \\ 0 & 1 \end{bmatrix}, \qquad \theta = k\pi h \, .$$

For $k = \frac{N}{2}$, $\hat{S}_{h,r}(\frac{\pi}{2})$ is a mapping from $\hat{b}_{\frac{N}{2}}$ onto itself and equals to 1. Similarly, a Jacobi relaxation operation operating at the black points only gives

$$\hat{S}_{h,b}(\theta) = \begin{bmatrix} 1 & 0 \\ \cos\theta & 0 \end{bmatrix} \quad 0 < \theta < \frac{\pi}{2} \, , \quad \text{and} \quad \hat{S}_{h,b}(\frac{\pi}{2}) = 0 \, . \tag{2.4}$$

Hence, the spectral representation of the red/black Gauss-Seidel iteration can be easily obtained as

$$\hat{S}_{h,r/b}(\theta) = \hat{S}_{h,b}(\theta)\, \hat{S}_{h,r}(\theta) = \begin{bmatrix} 0 & \cos\theta \\ 0 & \cos^2\theta \end{bmatrix} \quad 0 < \theta < \frac{\pi}{2} \, , \quad \text{and} \quad \hat{S}_{h,r/b}(\frac{\pi}{2}) = 0 \, .$$

2.2 A two-color multigrid direct solver

Now, let us study the coarse-grid corrector K_h^{2h} by using the basis $(\hat{r}_k, \hat{b}_k)^T$. Let the restriction operator I_h^{2h} and the interpolation operator I_{2h}^h be

$$I_h^{2h}: \quad \left| \frac{1}{4}, \frac{1}{2}, \frac{1}{4} \right|_h^{2h} \quad \text{and} \quad I_{2h}^h: \quad \left| c, 1, c \right|_{2h}^h, \tag{2.5}$$

where c is an arbitrary constant. Since points of the coarse grid coincide exactly with red points of the fine grid for the 1D case, $\hat{I}_h^{2h}(\theta)$, which is a mapping from $(\hat{r}_k,\hat{b}_k)^T$ to $\hat{r}_k$, and $\hat{I}_{2h}^h(\theta)$, a mapping from $\hat{r}_k$ to $(\hat{r}_k,\hat{b}_k)^T$, assume the following simple forms,

$$\hat{I}_h^{2h}(\theta) = \left[\frac{1}{2}, \frac{\cos\theta}{2} \right] \quad \text{and} \quad \hat{I}_{2h}^h(\theta) = \begin{bmatrix} 1 \\ 2c\cos\theta \end{bmatrix}.$$

In the red/black spectral domain, the $2h$-grid, the h-grid discretized Laplacian operators and the identity matrix are represented respectively by

$$\hat{L}_{2h}(\theta) = \frac{2(\cos 2\theta - 1)}{(2h)^2}, \quad \hat{L}_h(\theta) = \frac{2}{h^2} \begin{bmatrix} -1 & \cos\theta \\ \cos\theta & -1 \end{bmatrix}, \quad \hat{I}_h(\theta) = \begin{bmatrix} 1 & 0 \\ 0 & 1 \end{bmatrix}.$$

Hence, we obtain

$$\hat{K}_h^{2h}(\theta) = \hat{I}_h(\theta) - \hat{I}_{2h}^h(\theta)\hat{L}_{2h}^{-1}(\theta)\hat{I}_h^{2h}(\theta)\hat{L}_h(\theta) = \begin{bmatrix} 0 & 0 \\ -2c\cos\theta & 1 \end{bmatrix}. \tag{2.6}$$

Equation (2.6) shows that all red computational waves are eliminated by the coarse-grid corrector K_h^{2h}. Suppose that we are able to eliminate the effect of all black computational waves by some smoothing operation. Then, one coarse-grid correction followed by such a smoothing operation is sufficient for solving the two-grid problem exactly. From (2.4), we know that a simple Jacobi iteration at the black points, i.e. $S_{h,b}$, serves this purpose. Consequently, by choosing

$$M_h^{2h} = S_{h,b}\, K_h^{2h}, \quad \text{with} \quad K_h^{2h} = I_h - I_{2h}^h L_{2h}^{-1} I_h^{2h} L_h, \tag{2.7}$$

$\hat{M}_h^{2h}(\theta)$ are 2×2 zero matrices for all $0<\theta<\frac{\pi}{2}$. Besides, $\hat{M}_h^{2h}(\frac{\pi}{2})$ is also zero. Thus, the two-grid method (2.7) is exact.

2.3 Modification and generalization

Although the above analysis is independent of the value c, the choice $c = 0$ saves computational work and, therefore, is preferable in practice. It is possible to reduce the computational work of (2.7) further by using $S_{h,r}$ or $S_{h,b}$ as presmoother. Depending on whether we use $S_{h,r}$ or $S_{h,b}$, the residues at the red or black points are zero, and in this case the restriction operator I_h^{2h} in (2.5) can be replaced either by

$$[\ \frac{1}{4}\ ,\ 0\ ,\ \frac{1}{4}\ ]_h^{2h} \qquad \text{or} \qquad [\ 0\ ,\ \frac{1}{2}\ ,\ 0\ ]_h^{2h}\ .$$

In particular, if we use $S_{h,b}$ as presmoother and let $c = 0$, a modified two-color two-grid direct solver can be described as follows:

(1) Perform a Jacobi iteration at black points.

(2) Calculate residues at the red points and multiply them by $\frac{1}{2}$.

(3) Solve the system of residue equations on the $2h$-grid and add the coarse-grid solution back to the original values at the red points.

(4) Perform a Jacobi iteration at black points.

This algorithm corresponds to the following two-grid operator

$$M_h^{2h} = S_{h,b}\ (\ I_{h,r} - L_{2h}^{-1}\frac{1}{2}L_{h,r}\ )\ S_{h,b}\ , \tag{2.8}$$

where $L_{h,r}$ is the restriction of the discretized Laplacian operator to the red points of the h-grid, and $I_{h,r}$ is the identity operator for the red points. For $0 < \theta < \frac{\pi}{2}$, the spectral representation of $L_{h,r}$ and $I_{h,r}$ is given by

$$\hat{L}_{h,r}(\theta) = \frac{2}{h^2}\begin{bmatrix} -1 & \cos\theta \\ 0 & 0 \end{bmatrix}, \qquad \hat{I}_{h,r}(\theta) = \begin{bmatrix} 1 & 0 \\ 0 & 0 \end{bmatrix}.$$

Note that the calculation of the residue takes the same amount of work as the smoothing operation at every grid point. We compute the residues at all grid points in (2.7) while we perform the smoothing operation at one half of the grid points and compute the residue at the other half of the grid points in (2.8). The saving comes from the fact that a 3-point averaging operation is needed by (2.7) and that only a multiplication of $\frac{1}{2}$ is required by (2.8). The saving in the restriction and interpolation procedures

will be generalized to the 2D case in Section 3.2.

A two-color L-grid direct solver ($L > 2$) can be defined by using the above two-color two-grid method recursively, i.e.

$$M_h^{2h} = S_{h,b} \left(I_{h,r} - X_{2h} \frac{1}{2} L_{h,r} \right) S_{h,b} , \tag{2.9a}$$

with

$$X_h = M_h^{2h} , h = \frac{1}{2^l} , 2 \le l \le L-1 , \quad \text{and} \quad X_h = L_h^{-1} , h = \frac{1}{2} . \tag{2.9b}$$

It can be proved by induction that (2.9) is a direct method for the system of equations (2.1).

There exists no analog of equation (2.6) for the 2D problem so that there is no 2D direct solver corresponding to the one described above. However, a relation similar to (2.6) holds in the low frequency region which means that the 2D coarse-grid corrector can reduce errors of low frequency components effectively.

3. Analysis and design of 2D multigrid algorithm

Consider the solution of the 5-point discretized Poisson equation,

$$\frac{1}{h^2}\left(u_{n_x-1,n_y} + u_{n_x+1,n_y} + u_{n_x,n_y-1} + u_{n_x,n_y+1} - 4\, u_{n_x,n_y} \right) = f_{n_x,n_y} \ , \quad 1 \le n_x, n_y \le N-1 \ , \tag{3.1}$$

where u_{n_x,n_y} is given for n_x, $n_y = 0$ or N, and $N = \frac{1}{h}$ is even, by a $(h,2h)$ two-grid method with the red/black Gauss-Seidel smoother. Similar to the 1D case, we can interpret the physical mechanism of this algorithm as the evolution of two computational waves. Since the same algorithm has been analyzed by Stüben and Trottenberg [9], our discussion emphasizes the physical interpretation associated to the two-color Fourier analysis, rather than the specific mathematical result derived.

3.1 2D two-color Fourier analysis

The errors e_{n_x,n_y} associated to (3.1) can be expanded as

$$e_{n_x,n_y} = \sum_{k_x=1}^{N-1} \sum_{k_y=1}^{N-1} \hat{e}_{k_x,k_y} \sin(k_x \pi n_x h) \sin(k_y \pi n_y h) \ .$$

We divide grid points with indices $\mathbf{n} = (n_x,n_y)$ into red and black points, depending on whether n_x+n_y is even or odd. Then, errors at red and black points define red and black sequences, which can be expanded as

$$e_{n_x,n_y} = \sum_{\mathbf{k} \in K_r} \hat{r}_{k_x,k_y} \sin(k_x \pi n_x h) \sin(k_y \pi n_y h) \ , \qquad n_x+n_y \quad \text{even} \ ,$$

$$e_{n_x,n_y} = \sum_{\mathbf{k} \in K_b} \hat{b}_{k_x,k_y} \sin(k_x \pi n_x h) \sin(k_y \pi n_y h) \ , \qquad n_x+n_y \quad \text{odd} \ ,$$

where $K_r = K$ and $K_b = K \cup \{ (\frac{N}{2} , \frac{N}{2}) \}$, and where

$$K = \{ (k_x,k_y) \in I^2 : \ k_x+k_y \le N-1 \ , \ k_x,k_y \ge 1 \quad \text{or} \quad k_y = N - k_x \ , \ 1 \le k_x \le \frac{N}{2}-1 \} \ ,$$

For $\mathbf{k} \in K$, we denote $(N-k_x,N-k_y)$ by $\mathbf{k}'$. It is straightforward to check that $\hat{r}_{\mathbf{k}}$, $\hat{b}_{\mathbf{k}}$, $\hat{e}_{\mathbf{k}}$, $\hat{e}_{\mathbf{k}'}$ are related via

$$\begin{bmatrix} \hat{r}_{\mathbf{k}} \\ \hat{b}_{\mathbf{k}} \end{bmatrix} = \frac{1}{2} \begin{bmatrix} 1 & 1 \\ 1 & -1 \end{bmatrix} \begin{bmatrix} \hat{e}_{\mathbf{k}} \\ \hat{e}_{\mathbf{k}'} \end{bmatrix} , \quad \mathbf{k} \in K \quad \text{and} \quad \hat{b}_{\mathbf{k}} = \hat{e}_{\mathbf{k}} \ , \quad \mathbf{k} = (\frac{N}{2},\frac{N}{2}) \ .$$

The original and the folded two-color Fourier domains are depicted in Figure 1. Note that K_r and K_b differs only by a single element $(\frac{N}{2},\frac{N}{2})$ and, therefore, at the frequency $(\frac{N}{2},\frac{N}{2})$ we have only a scalar $\hat{b}_{\frac{N}{2},\frac{N}{2}}$. As before, we define $\theta = (\theta_x,\theta_y) = (k_x\pi h, k_y\pi h)$ and Θ denotes the set of θ whose corresponding $\mathbf{k}$ belongs to K.

For the moment we consider the two-grid iteration matrix with one red/black Gauss-Seidel iteration

$$M_h^{2h} = K_h^{2h} S_{h,r/b} \quad (\text{ or } S_{h,r/b} K_h^{2h}), \qquad K_h^{2h} = I_h - I_{2h}^h L_{2h}^{-1} I_h^{2h} L_h, \tag{3.2}$$

where L_h and L_{2h} are the 5-point discretizations of the Laplacian on the h and $2h$ grids, and I_h^{2h} and I_{2h}^h are the full-weighting restriction and linear interpolation operators, given by

$$I_h^{2h}: \left|\begin{array}{ccc} \frac{1}{16} & \frac{1}{8} & \frac{1}{16} \\ \frac{1}{8} & \frac{1}{4} & \frac{1}{8} \\ \frac{1}{16} & \frac{1}{8} & \frac{1}{16} \end{array}\right|_h^{2h}, \tag{3.3a}$$

and

$$I_{2h}^h: \left|\begin{array}{ccc} \frac{1}{4} & \frac{1}{2} & \frac{1}{4} \\ \frac{1}{2} & 1 & \frac{1}{2} \\ \frac{1}{4} & \frac{1}{2} & \frac{1}{4} \end{array}\right|_{2h}^{h}. \tag{3.3b}$$

The problem is to determine the spectral radius $\rho(M_h^{2h})$ of the two-grid iteration matrix.

Each of the 4×4 frequency domain matrices appearing below corresponds to a mapping from a vector space formed by the vector

$$(r_{\mathbf{k}}, -r_{\bar{\mathbf{k}}}, b_{\mathbf{k}}, -b_{\bar{\mathbf{k}}})^T,$$

onto itself, where

$$\mathbf{k} = (k_x,k_y) \quad 1 \le k_x,k_y < \frac{N}{2}, \quad \bar{\mathbf{k}} = \begin{cases} (N-k_x,k_y) & \text{if } k_x \ge k_y \\ (k_x,N-k_y) & \text{if } k_x < k_y \end{cases}.$$

We also use the abbreviations

$$\alpha = \frac{\cos\theta_x+\cos\theta_y}{2}\ , \quad \tilde{\alpha} = \frac{\cos\tilde{\theta}_x+\cos\tilde{\theta}_y}{2}\ , \quad \beta = \cos\theta_x\cos\theta_y\ , \quad \tilde{\beta} = \cos\tilde{\theta}_x\cos\tilde{\theta}_y\ .$$

(1) Smoothing

For $\theta_x\ , \theta_y < \frac{\pi}{2}$, the frequency domain matrix corresponding to the red/black Gauss-Seidel iteration is

$$\hat{S}_{h,r/b}(\theta) = \hat{S}_{h,b}(\theta)\,\hat{S}_{h,r}(\theta) = \begin{bmatrix} I & 0 \\ J & 0 \end{bmatrix}\begin{bmatrix} 0 & J \\ 0 & I \end{bmatrix} = \begin{bmatrix} 0 & J \\ 0 & J^2 \end{bmatrix}, \tag{3.4}$$

where 0 is the 2×2 zero matrix, I is the 2×2 identity matrix, and

$$J = \begin{bmatrix} \alpha & 0 \\ 0 & \tilde{\alpha} \end{bmatrix}.$$

When θ_x or θ_y is equal to $\frac{\pi}{2}$, $\hat{S}_{h,r/b}$ is a 2×2 matrix

$$\hat{S}_{h,r/b}(\theta) = \begin{bmatrix} 0 & \alpha \\ 0 & \alpha^2 \end{bmatrix},$$

which is a mapping from $(\hat{r}_{\mathbf{k}},\hat{b}_{\mathbf{k}})^T$ to $(\hat{r}_{\mathbf{k}},\hat{b}_{\mathbf{k}})^T$. Finally, for $\theta_x = \theta_y = \frac{\pi}{2}$, $\hat{S}_{h,r/b} = 0$, which is a mapping from $\hat{b}_{\mathbf{k}}$ to itself.

Note that when the first partial step of the red/black Gauss-Seidel iteration, i.e. the Jacobi iteration at red points, is performed, the original values of the red points are discarded and, hence, the computational process that follows is only determined by the initial values of the black points. This observation is the basis for reducing the two-color analysis to a one-color analysis.

(2) Coarse-grid correction

Let us first consider the case $\theta_x\ , \theta_y < \frac{\pi}{2}$. The frequency domain matrices for operators I_h, L_h and L_{2h}^{-1} in (3.2) can be written as

$$\hat{I}_h(\theta) = \begin{bmatrix} I & 0 \\ 0 & I \end{bmatrix}, \quad \hat{L}_h(\theta) = \frac{4}{h^2}\begin{bmatrix} -I & J \\ J & -I \end{bmatrix}, \quad \hat{L}_{2h}^{-1}(\theta) = \frac{h^2}{2\delta}\ , \ \delta = 2\alpha^2-\beta-1\ . \tag{3.5}$$

In (3.4) and (3.5), there is no coupling between vectors $(\hat{r}_{\mathbf{k}},\hat{b}_{\mathbf{k}})^T$ and $(\hat{r}_{\tilde{\mathbf{k}}},\hat{b}_{\tilde{\mathbf{k}}})^T$. The coupling between them comes from the full-weighting restriction and linear

interpolation operations, which are more complicated than in the 1D case since the coarse-grid points do not coincide any longer with the red points of the h-grid.

The decomposition, shown in Figure 2 and commonly used in the multirate signal processing context [4], is very useful for understanding the physical mechanism of interpolation and restriction operators, and for deriving their frequency domain matrices. Conceptually, we decompose the restriction procedure into two steps.

Step 1: lowpass filtering (or averaging) at every point of Ω_h, where the weighting coefficients are specified by stencil (3.3a).

Step 2: down-sampling (or injecting) values from Ω_h to Ω_{2h}.

The interpolation operator I_{2h}^h is also decomposed into two steps.

Step 1: up-sampling values from Ω_{2h} to Ω_h, by which we assign 0 to points which belong to $\Omega_h - \Omega_{2h}$

Step 2: lowpass filtering at every point of Ω_h, where the weighting coefficients are specified by stencil (3.3b).

It is relatively easy to find a frequency domain matrix representation for each of the above steps. Combining them together, we obtain

$$\hat{I}_h^{2h}(\theta) = [1 \;\; 1 \;\; 0 \;\; 0] \times \frac{1}{4} \begin{bmatrix} 1+\beta & 0 & 2\alpha & 0 \\ 0 & 1+\bar{\beta} & 0 & 2\bar{\alpha} \\ 2\alpha & 0 & 1+\beta & 0 \\ 0 & 2\bar{\alpha} & 0 & 1+\bar{\beta} \end{bmatrix} = \frac{1}{4}[1+\beta \;\; 1+\bar{\beta} \;\; 2\alpha \;\; 2\bar{\alpha}], \qquad (3.6a)$$

and

$$\hat{I}_{2h}^h(\theta) = \begin{bmatrix} 1+\beta & 0 & 2\alpha & 0 \\ 0 & 1+\bar{\beta} & 0 & 2\bar{\alpha} \\ 2\alpha & 0 & 1+\beta & 0 \\ 0 & 2\bar{\alpha} & 0 & 1+\bar{\beta} \end{bmatrix} \times \frac{1}{2} \begin{bmatrix} 1 \\ 1 \\ 0 \\ 0 \end{bmatrix} = \frac{1}{2} \begin{bmatrix} 1+\beta \\ 1+\bar{\beta} \\ 2\alpha \\ 2\bar{\alpha} \end{bmatrix}. \qquad (3.6b)$$

Thus, in the frequency domain, the down-sampling operation adds the high frequency component $-\hat{r}_{\tilde{\mathbf{k}}}$ to the low frequency component $\hat{r}_{\mathbf{k}}$. This phenomenon is known as *aliasing* [4]. On the other hand, the up-sampling operation duplicates the low fre-

quency component $\hat{f}_{\mathbf{k}}$ in the high frequency region in the form of $-\hat{f}_{\tilde{\mathbf{k}}}$, which is called *imaging* [4]. The lowpass filters cascaded with the down-sampling and the up-sampling operators are basically used to reduce the aliasing and imaging effects. For example, when θ_x and θ_y are close to 0, $\alpha \approx 1$, $\beta \approx 1$, $\tilde{\alpha} \approx 0$, and $\tilde{\beta} \approx -1$. Hence, the aliasing and imaging effects occurring between $(\hat{f}_{\mathbf{k}}, \hat{b}_{\mathbf{k}})^T$ and $(\hat{f}_{\tilde{\mathbf{k}}}, \hat{b}_{\tilde{\mathbf{k}}})^T$ are substantially eliminated by the associated lowpass filters.

The product $\hat{I}_{2h}^{h}(\theta)\hat{I}_{h}^{2h}(\theta)$ can be expressed as

$$\hat{I}_{2h}^{h}(\theta)\hat{I}_{h}^{2h}(\theta)=\frac{1}{8}\begin{bmatrix} F_{11} & F_{12} \\ F_{21} & F_{22} \end{bmatrix}, \quad \text{where} \quad F_{11}=\begin{bmatrix} (1+\beta)^2 & (1+\beta)(1+\tilde{\beta}) \\ (1+\beta)(1+\tilde{\beta}) & (1+\tilde{\beta})^2 \end{bmatrix}, \tag{3.7}$$

$$F_{12}=F_{21}^{T}=\begin{bmatrix} 2\alpha(1+\beta) & 2\tilde{\alpha}(1+\beta) \\ 2\alpha(1+\tilde{\beta}) & 2\tilde{\alpha}(1+\tilde{\beta}) \end{bmatrix}, \qquad F_{22}=\begin{bmatrix} 4\alpha^2 & 4\alpha\tilde{\alpha} \\ 4\alpha\tilde{\alpha} & 4\tilde{\alpha}^2 \end{bmatrix}.$$

Therefore, from (3.5) and (3.7), we obtain the coarse-grid corrector,

$$\hat{K}_{h}^{2h}(\theta)=\begin{bmatrix} K_{11} & K_{12} \\ K_{21} & K_{22} \end{bmatrix},$$

where

$$K_{11}=I-\frac{1}{4\delta}(F_{12}J-F_{11}), \qquad K_{22}=I-\frac{1}{4\delta}(F_{21}J-F_{22}),$$

$$K_{12}=\frac{-1}{4\delta}(F_{11}J-F_{12}), \qquad K_{21}=\frac{-1}{4\delta}(F_{22}J-F_{21}),$$

which holds for $\theta_x, \theta_y < \frac{\pi}{2}$. For the remaining cases, we can show that $\hat{K}_{h}^{2h}(\theta)$ is either the 2×2 identity matrix or 1, depending on whether only one of θ_x, θ_y is $\frac{\pi}{2}$ or both θ_x and θ_y are $\frac{\pi}{2}$.

(3) Two-grid iteration

Combining results in the previous discussion, we find that in the frequency domain $M_h^{2h} = K_h^{2h} S_{h,r/b}$ is represented as

$$\hat{M}_{h}^{2h}(\theta)=\begin{bmatrix} 0 & K_{11}J+K_{12}J^2 \\ 0 & K_{21}J+K_{22}J^2 \end{bmatrix}, \qquad \theta_x, \theta_y < \frac{\pi}{2}, \tag{3.8a}$$

$$\hat{M}_h^{2h}(\theta) = \begin{bmatrix} 0 & \alpha \\ 0 & \alpha^2 \end{bmatrix}, \qquad \theta_x \text{ or } \theta_y = \frac{\pi}{2}, \tag{3.8b}$$

$$\hat{M}_h^{2h}(\theta) = 0, \qquad \theta_x = \theta_y = \frac{\pi}{2}. \tag{3.8c}$$

Therefore, the spectral radius of $\hat{M}_h^{2h}(\theta)$ is

$$\rho(\hat{M}_h^{2h}(\theta)) = \begin{cases} \rho(K_{21}J+K_{22}J^2) & \theta_x, \theta_y < \frac{\pi}{2} \\ \alpha^2 & \theta_x \text{ or } \theta_y = \frac{\pi}{2} \\ 0 & \theta_x = \theta_y = \frac{\pi}{2} \end{cases}, \tag{3.9}$$

and finally the spectral radius of the two-grid iteration matrix is

$$\rho(M_h^{2h}) = \max_{\theta_x,\theta_y \le \frac{\pi}{2}} \rho(\hat{M}_h^{2h}(\theta)) .$$

The two-to-one color reduction is mathematically clear from equations (3.8) and (3.9). Note that the two-grid iteration process $M_h^{2h}(\theta)$ is the combination of two processes

$$M_{12}(\theta) = K_{11}J+K_{12}J^2, \qquad M_{22}(\theta) = K_{21}J+K_{22}J^2,$$

which describe the evolution from $(b_{\mathbf{k}},-b_{\tilde{\mathbf{k}}})^T$ to $(r_{\mathbf{k}},-r_{\tilde{\mathbf{k}}})^T$ and $(b_{\mathbf{k}},-b_{\tilde{\mathbf{k}}})^T$ respectively. Since the m-fold repetition of M_h^{2h} gives

$$[(\hat{M}_h^{2h}(\theta))^m]_{12} = M_{12}(\theta)\, M_{22}^{m-1}(\theta), \qquad [(\hat{M}_h^{2h}(\theta))^m]_{22} = M_{22}^m(\theta),$$

the convergence of the two-grid method depends entirely on the process $M_{22}(\theta)$.

The above derivation can be easily generalized to the case with more than one red/black Gauss-Seidel smoothing operation. Suppose that ν_1 and ν_2 such smoothing operations are used respectively for the presmoother and postsmoother, then

$$\rho[M_h^{2h}(\nu_1,\nu_2)] = \rho(S_{h,r/b}^{\nu_2} K_h^{2h} S_{h,r/b}^{\nu_1}) = \rho(K_h^{2h} S_{h,r/b}^{\nu_1+\nu_2}),$$

where the last equality comes from the fact $\rho(AB) = \rho(BA)$, and

$$\rho(\hat{M}_h^{2h}(\nu_1,\nu_2,\theta)) = \begin{cases} \rho(K_{21}J^{2\nu-1}+K_{22}J^{2\nu}) & \theta_x, \theta_y < \frac{\pi}{2} \\ \alpha^{2\nu} & \theta_x \text{ or } \theta_y = \frac{\pi}{2} \\ 0 & \theta_x = \theta_y = \frac{\pi}{2} \end{cases},$$

where $\nu = \nu_1 + \nu_2$.

Let us examine the matrix

$$M_{eq} = K_{21}J^{2\nu-1} + K_{22}J^{2\nu} ,$$

which represents a one-color two-grid iteration process and can be expressed as

$$M_{eq} = JK_{eq}J^{2\nu-1} ,$$

where

$$K_{eq} = I - \frac{1}{4\delta}J^{-1}F_{21}(J^2 - I) = \begin{bmatrix} 1 - \frac{(1+\beta)(\alpha^2-1)}{2\delta} & -\frac{(1+\beta)(\bar{\alpha}^2-1)}{2\delta} \\ -\frac{(1+\beta)(\alpha^2-1)}{2\delta} & 1 - \frac{(1+\beta)(\bar{\alpha}^2-1)}{2\delta} \end{bmatrix}$$

is the equivalent one-color coarse-grid corrector. Since $\rho(JK_{eq}J^{2\nu-1}) = \rho(K_{eq}J^{2\nu})$, we see that J^2 can be viewed as the equivalent one-color smoother S_{eq}, which corresponds to two Jacobi relaxation steps for the black component b_k.

Although our analysis is different from that of Stüben and Trottenberg [9], it turns out, without surprise, that they are mathematically equivalent and lead to the same results. In [9], Stüben and Trottenberg reduced their analysis to the determination of the largest value among all the spectral radii of matrices $J^{2\nu}K_{eq}$, $0 < \theta_x, \theta_y < \frac{\pi}{2}$, and a closed form of this quantity has been derived (pp. 104-108). Since the same result holds here, we summarize it as follows

$$\rho[\, M_h^{2h}(\nu=\nu_1+\nu_2)\,] = \begin{cases} \frac{1}{4} & \nu = 1 \\ \frac{1}{2\nu}\left(\frac{\nu}{\nu+1}\right)^{\nu+1} & \nu \geq 2 \end{cases}$$

In the above expression, the maximum of $\rho[\hat{M}_h^{2h}(\theta)]$ occurs at $\theta = (\frac{\pi}{2},0)$ or $(0,\frac{\pi}{2})$ when $\nu = 1$ and at $(\cos^{-1}[(\frac{\nu}{\nu+1})^{1/2}] , \cos^{-1}[(\frac{\nu}{\nu+1})^{1/2}])$ when $\nu \geq 2$.

3.2 Rearrangement of the smoothing order

Suppose that we rearrange the smoothing order from { red $\rightarrow$ black } to { black $\rightarrow$ red } for the two-grid iteration discussed before. In the frequency domain, the black/red Gauss-Seidel iteration matrix becomes

$$\hat{S}_{h,b/r}(\boldsymbol{\theta}) = \begin{bmatrix} J^2 & 0 \\ J & 0 \end{bmatrix} \theta_x,\theta_y < \frac{\pi}{2}; \quad \begin{bmatrix} \alpha^2 & 0 \\ \alpha & 0 \end{bmatrix}, \theta_x \text{ or } \theta_y = \frac{\pi}{2}; \quad 0, \theta_x=\theta_y=\frac{\pi}{2} .$$

This indicates that the computational process that follows is determined by the initial values of the red points only. Several facts can be obtained by modifying the derivation in the previous section slightly. The two-grid method with black/red Gauss-Seidel relaxation consists of two processes

$$M_{11}(\theta) : (r_{\mathbf{k}},-r_{\bar{\mathbf{k}}})^T \rightarrow (r_{\mathbf{k}},-r_{\bar{\mathbf{k}}})^T , \quad M_{21}(\theta) : (r_{\mathbf{k}},-r_{\bar{\mathbf{k}}})^T \rightarrow (b_{\mathbf{k}},-b_{\bar{\mathbf{k}}})^T .$$

Asymptotically, its rate of convergence is determined by that of the process $M_{11}(\theta)$. In mathematical terms, we have

$$\rho[\, \hat{K}_h^{2h}(\theta)\, \hat{S}_{h,b/r}^{\nu}(\theta)\,] = \begin{cases} \rho(K_{12}J^{2\nu-1}+K_{11}J^{2\nu}) & \theta_x\,,\ \theta_y < \dfrac{\pi}{2} \\ \alpha^{2\nu} & \theta_x \text{ or } \theta_y = \dfrac{\pi}{2} \\ 0 & \theta_x = \theta_y = \dfrac{\pi}{2} \end{cases} .$$

Since $F_{12} = F_{21}^T$, we obtain the equality

$$\rho(K_{12}J^{2\nu-1}+K_{11}J^{2\nu}) = \rho(K_{21}J^{2\nu-1}+K_{22}J^{2\nu}) ,$$

which implies that the spectral radii of the two-grid methods with either the red/black or black/red Gauss-Seidel relaxation are the same.

Motivated by the 1D algorithm (2.8), we consider an improved multigrid method whose two-grid iteration operator $M_{h,i}^{2h}$ is of the form

$$M_{h,i}^{2h} = S_{h,b}\ K_{h,i}^{2h}\ S_{h,r} , \qquad K_{h,i}^{2h} = I_{h,r} - I_{2h}^{r} L_{2h}^{-1} I_{b}^{2h} L_{h,b} ,$$

where $I_{h,r}$ is the identity operator at red points, $L_{h,b}$ is the restriction of the 5-point discretized Laplacian operator to the black points of Ω_h, and I_b^{2h} and I_{2h}^r are the

black-to-coarse restriction and coarse-to-red interpolation operators defined by,

$$I_b^{2h}: \left| \begin{array}{ccc} 0 & \frac{1}{8} & 0 \\ \frac{1}{8} & 0 & \frac{1}{8} \\ 0 & \frac{1}{8} & 0 \end{array} \right|_b^{2h}, \quad \text{and} \quad I_{2h}^r: \left| \begin{array}{ccc} \frac{1}{4} & 0 & \frac{1}{4} \\ 0 & 1 & 0 \\ \frac{1}{4} & 0 & \frac{1}{4} \end{array} \right|_{2h}^r . \tag{3.10}$$

Comparing (3.3) and (3.10), we see that the simplified restriction operator I_b^{2h} and interpolation operator I_{2h}^r are in fact obtained respectively by setting the coefficients of the red points of the full weighting operator I_h^{2h} and of the black points of the linear interpolation operator I_{2h}^h equal to 0. This change is motivated by the observation that

$$S_{h,b}\ K_h^{2h}\ S_{h,r} = S_{h,b}\ K_{h,i}^{2h}\ S_{h,r}\ ,$$

since the residues at the red points are zero before the restriction operation and the values at the black points are not used after the interpolation. The corresponding computational algorithm is stated below.

(1) Perform a Jacobi iteration at the red points.
(2) Calculate residues at the black points and average them with the coefficients specified by I_b^{2h} to obtain residue values at the coarse-grid points.
(3) Solve the system of residue equations on the $2h$-grid, and interpolate the coarse-grid solution to the red points according to I_{2h}^r, which is then added back to the original values at the red points.
(4) Perform a Jacobi iteration at the black points.

One important feature of the improved method is that it splits one complete iteration $S_{h,r}\ S_{h,b}$ into two separate operations and uses $S_{h,r}$ and $S_{h,b}$ as presmoother and postsmoother respectively. It is this particular arrangement that makes possible the reduction of computational work associated to the use of the simplified restriction and interpolation operators (3.10). The improved method has the same convergence rate as the conventional method using either red/black or black/red Gauss-Seidel relaxation, since

$$\rho(S_{h,b}\ K_{h,i}^{2h}\ S_{h,r}) = \rho(S_{h,b}\ K_h^{2h}\ S_{h,r}) = \rho(K_h^{2h}\ S_{h,b/r}\ ) = \rho(K_h^{2h}\ S_{h,r/b}\ ) .$$

The generalization of the improved method to $\nu \geq 2$ is straightforward. The key is to position $S_{h,r}$ just before the residue restriction step and $S_{h,b}$ just after the solution interpolation step. For example, when $\nu = 2$, the improved two-grid methods can be

$$S_{h,b/r}\, K_{h,i}^{2h}\, S_{h,b/r}\,, \qquad S_{h,b}\, K_{h,i}^{2h}\, S_{h,r}\, S_{h,r/b}\,, \quad \text{or} \quad S_{h,r/b}\, S_{h,b}\, K_{h,i}^{2h}\, S_{h,r}\,.$$

4. Conclusions

A two-color Fourier analysis has been proposed to analyze the multigrid method with red/black Gauss-Seidel smoothing for the model Poisson problem. By this analysis, we can clearly explain the coupling phenomenon existing between the low and high wavenumber components of the solution, give an more intuitive derivation of the two-grid analysis, and derive some variants of this algorithm. The same analytical approach can also be conveniently applied to the MGR-CH (Multigrid Reduction with checkered Gauss-Seidel relaxations) method [5][8].

Acknowledgement

The authors would like to thank Dr. Shlomo Ta'asan for several helpful discussions.

References

1. L. Adams and H. F. Jordan, "Is SOR color-blind," *SIAM J. Sci. Stat.*, vol. 7, no. 2, Apr. 1986.
2. A. Brandt, "Multigrid solvers on parallel computers," in *Elliptic Problem Solvers*, ed. M. H. Schultz, pp. 39-83, Academic Press, Inc., New York, N.Y., 1981.
3. A. Brandt, "Guide to multigrid development," in *Multigrid Methods*, ed. W. Hackbusch and U. Trottenberg, pp. 220-312, Springer-Verlag, New York, N.Y., 1982.
4. R. E. Crochiere and L. R. Rabiner, *Multirate Digital Signal Processing*, Prentice-Hall, Inc., Englewood Cliffs, N.J., 1983.
5. H. Foerster, K. Stüben, and U. Trottenberg, "Nonstandard multigrid techniques using checkered relaxation and intermediate grids," in *Elliptic Problem Solvers*, ed. M. Schultz, pp. 285-300, Academic Press, Inc., New York, N.Y., 1981.
6. W. Hackbusch, *Multi-Grid Methods and Applications*, Springer-Verlag, Berlin, Germany, 1985.
7. C.-C. J. Kuo, B. C. Levy, and B. R. Musicus, "A local relaxation method for solving elliptic PDEs on mesh-connected arrays," *SIAM J. Sci. Stat. Comput.*, vol. 8, no. 4, pp. 550-573, Jul. 1987.
8. M. Ries, U. Trottenberg, and G. Winter, "A note on MGR methods," *Linear Algebra and Its Application*, vol. 49, pp. 1-26, 1983.
9. K. Stüben and U. Trottenberg, "Multigrid methods : fundamental algorithms, model problem analysis, and applications," in *Multigrid Methods*, ed. W. Hackbusch and U. Trottenberg, pp. 1-176, Springer-Verlag, New York, N.Y., 1982.

Figure Captions

Figure 1: (a) Conventional and (b) folded two-color Fourier domains.

Figure 2: Decomposition of the (a) restriction and (b) interpolation operators.

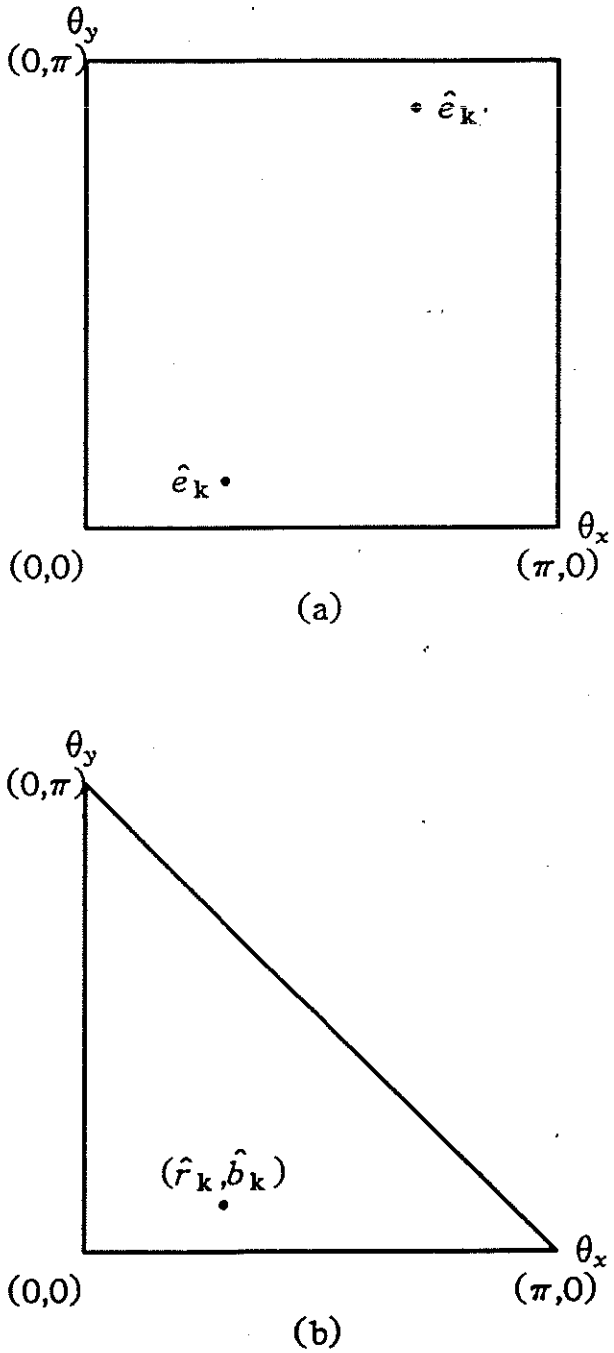

Figure 1: (a) Conventional and (b) folded two-color Fourier domains.

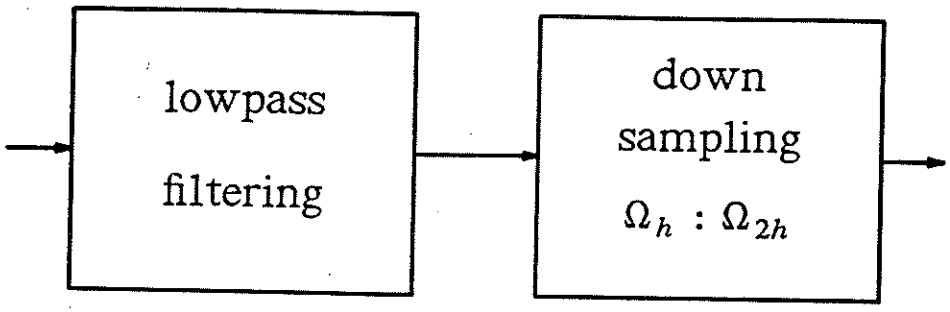

(a)

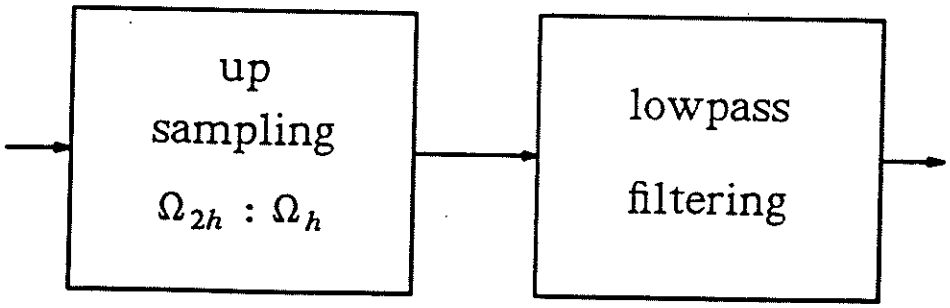

(b)

Figure 2: Decomposition of the (a) restriction and (b) interpolation operators.